32nd Annual International Conference of the IEEE EMBS
Buenos Aires, Argentina, August 31 - September 4, 2010

Ultrasonographic Characterization and Identification of Symptomatic Carotid Plaques

José Seabra, Luís Mendes Pedro (MD), José Fernandes e Fernandes (MD) and João Sanches

Abstract— **Carotid plaques are the main cause of neurological symptoms due to distal embolization or flow reduction. An objective classification of such lesions into symptomatic or asymptomatic is crucial for optimal treatment planning.**

The paper proposes a diagnostic framework to tackle this problem which consists of image processing, plaque detection, feature extraction and classification using AdaBoost in B-mode ultrasound (BUS) images. Image processing includes grey-level normalization, envelope Radio-Frequency (eRF) image retrieval, de-speckling and speckle extraction early proposed by the authors. The estimated images are used to extract a set of echo-morphology and texture features which are fused with clinical information provided by the physician.

The classification performance, assessed by means of the Leave-One-Patient-Out (LOPO) cross-validation technique applied to a population of 44 symptomatic and 102 asymptomatic plaques, yields 99.2% overall accuracy and 100% sensitivity in classifying symptomatic vs. asymptomatic plaques. Feature analysis and comparison of classification results obtained with different feature sets suggest the usefulness of an extended feature set here proposed for the identification of symptomatic plaques among the traditional ones used in the literature.

I. INTRODUCTION

Carotid plaques represent the primary cause of stroke which is the third leading cause of death in most industrialized countries. Among patients with such lesions, only a few show warning events, whereas the majority present cerebral events associated with previously asymptomatic plaques.

Several trials reported the significance of the degree of stenosis as a major indicator of stroke in both symptomatic and asymptomatic groups. Moreover, these studies have shown that surgical removal of plaques (endarterectomy) associated with a degree of stenosis of more than 70% resulted in an absolute reduction of 17% in the risk of ipsilateral stroke after 2 years and 11.6% at 3 years [1,2]. These observations indicate that not all the carotid plaques showing significant degree of stenosis are harmful and as carotid endarterectomy carries a considerable risk for the patient, an optimized characterization and identification of symptomatic plaques must be carried out. As suggested by histopathological studies, other factors such as plaque structure and echo-morphology (information on plaque grey-scale intensities) have shown to correlate with neurological symptoms [3,4]. In [5], surface disruption, severe stenosis, plaque heterogeneity and presence of juxta-luminal echolucent area were parameters associated with high morbidity. Studies aiming at quantitatively characterize carotid plaques include the computation of the grey scale median (GSM) from BUS images [5], the use of first and second order statistics [6], Fourier power spectrum [6] and Law's texture energy [7]. Moreover, the importance of the speckle present in BUS images as well as its statistical modeling for tissue characterization has been reported [8]. Here, a recently proposed algorithm [9] is used to estimate the de-speckled (speckle-free) and speckle images while it is argued that such fields are, respectively, sources of echo-morphology and texture information useful for plaque characterization.

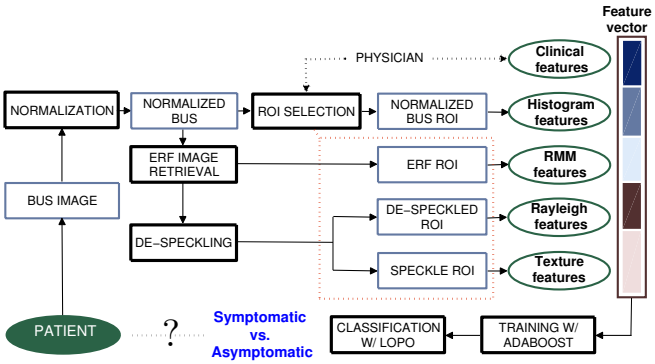

Fig. 1. Plaque classification framework.

The purpose of the paper is two-fold: (i) to build a plaque classification framework which uses a wide set of features, gathering clinical information as well as echo-morphology and texture parameters extracted after application of the de-speckling algorithm, and (ii) to determine the relative significance of the computed features in identifying symptoms in carotid plaques.

II. METHODS

In this section we describe the plaque classification framework (Fig. 1) which requires image normalization, estimation of the eRF image, de-speckling and speckle extraction. Using the computed images, a wide set of features is extracted from a region of interest (ROI) - plaque - outlined by the physician and used to train a classifier.

Data include 146 carotid bifurcation plaques from 99 patients, 75 males and 24 females. Mean age was 68 years old (41-88). Patients were observed consecutively through neurological consultation which included non-invasive examination with color-flow duplex scan of one or both carotids. A plaque was considered symptomatic when *Amaurosis fugax* or focal transitory, reversible or established neurological symptoms in the ipsilateral carotid territory, were observed

This work was supported by the Portuguese Government – FCT (ISR/IST plurianual funding).

J.Seabra and J.Sanches are with Institute for Systems and Robotics, Technical Superior Institute, Av. Rovisco Pais, 1049−001 Lisbon, Portugal. Corresponding author: jseabra@isr.ist.utl.pt

L.M.Pedro and J.F. Fernandes are with the Cardiovascular Institute of Lisbon and Hospital de Santa Maria, 1649-035 Lisbon, Portugal

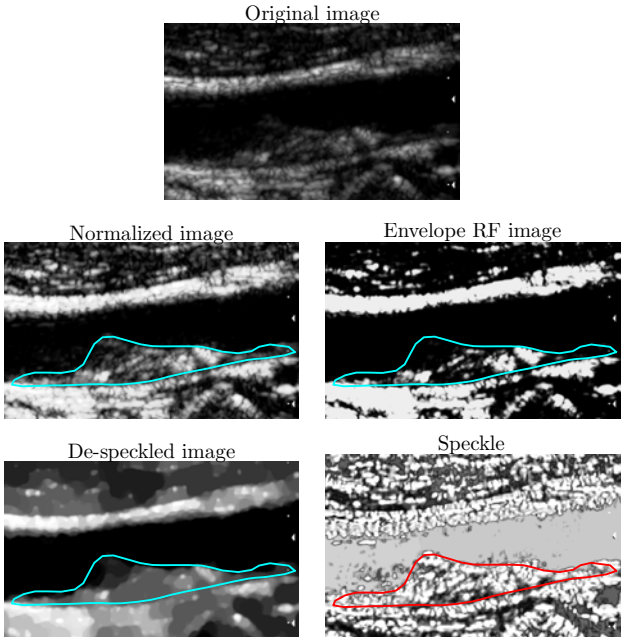

Fig. 2. Image processing consisting of normalization, eRF image estimation and computation of de-speckled and speckle images.

in the previous 6 months. 102 plaques were identified as asymptomatic while 44 have shown symptoms.

Image normalization is an important step to guarantee that images acquired under different conditions yield comparable and reproducible features and classification results. Image normalization was achieved as previously reported [4]; hence, the image intensities were linearly scaled so that the adventitia and blood intensities would be in the range of 190-195 and 0-5, respectively (Fig. 2).

The normalized image is used to segment existing plaque(s) in the image. Each plaque is delineated by drawing around its structure and the obtained contour is evenly re-sampled and smoothed using spline interpolation.

De-speckled and Speckle images, needed to compute the echo-morphology and texture features, are computed from the normalized BUS images. In a first step, the eRF image is estimated from the normalized BUS according to [10]. In a second step, the estimated eRF image is used to compute the speckle-free and speckle components, displayed in Fig. 2. This second step uses a Bayesian framework with the *Maximum a Posteriori* (MAP) criterion where the pixels are considered independent random variables with Rayleigh distribution, as described in [9].

Feature extraction is required to train the classifier. Features are obtained from clinical information provided by the physician and objective echo-morphology and texture parameters automatically computed from the normalized BUS, eRF, de-speckled and speckle images.

1) Clinical features: given by an experimented physician during consultation. The 4-element vector of clinical features include: (i) *evidence of plaque disruption*, defined by an interruption in the echogenic surface of the plaque; (ii) *presence of fibrous cap*, identified as an echogenic line over the structure of the plaque; (iii) *the degree of steno-sis*, quantified using cross-section area measurement combined with hemodynamic assessment, and (iv) *plaque echo-structure appearance*, where uniform plaques are defined as homogeneous while plaques presenting significant areas of echolucency are defined as heterogeneous.

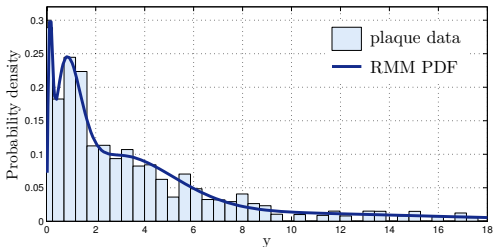

Fig. 3. RMM applied to plaque intensities in the eRF image: the RMM PDF is obtained as in (1) using the estimated *weights* and *Rayleigh* parameters.

2) Histogram features: extracted from the histogram of normalized pixel intensities inside the plaque. Hence, 13 histogram features are estimated, including the *mean grey value*, *median grey value*, *percentage of pixels with grey value lower than 40*, *standard deviation of grey values*, *kurtosis*, *skewness*, *energy*, *entropy*, *10-, 25-, 50-, 75- and 90- percentiles*.

3) RMM features: plaque echo-morphology may present different regions of echogenicity. In a recent publication [11], the authors proposed to use a mixture of Rayleigh distributions, known as Rayleigh Mixture Model (RMM) for modeling the plaque echo-morphology. The application of RMM is made on the eRF image, which can be approximated by Rayleigh statistics. Pixel intensities inside the plaque are considered random variables described by the following mixture of K distributions:

$$p(y_i|\mathbf{\Psi}) = \sum_{k=1}^{K} \theta_k p(y_i|\sigma_k), \qquad (1)$$

where $p(y_i|\sigma_k)$ is the Rayleigh probability density function (PDF). θ_k and σ_k are the weights and Rayleigh parameters of the mixture, respectively, which are estimated using the *Expectation-Maximization* method and $K = 6$ (see Fig. 3). Hence, we get a 13-element feature vector, consisting of 6 *mixture weights*, 6 *Rayleigh parameters* and the *effective number of RMM components*, determined by the number of mixture components with non-zero weight.

4) Rayleigh features: the de-speckled image is used to compute average theoretical estimators of the Rayleigh distribution inside the plaque region, including the *mean*, $\sigma_\mu = \overline{\sigma_{i,j}}\sqrt{\frac{\pi}{2}}$, *median*, $\sigma_\upsilon = \overline{\sigma_{i,j}}\sqrt{2\log(2)}$, *variance*, $\sigma_\sigma = \overline{\sigma_{i,j}}\sqrt{\frac{4-\pi}{2}}$ of *Rayleigh values* and *percentage of pixels with Rayleigh value lower than 40*, $\sigma_{PP40} = 100 - e^{-40^2/2\overline{\sigma_{i,j}}^2}$.

5) Texture features: involves the study of the spatial distribution of grey levels inside the plaque region extracted from the speckle image. These features are estimated from grey level co-occurrence matrices (GLCM), Autoregressive models (ARM) and Wavelet models. GLCMs are constructed using the relative frequencies $P(i, j, d, \theta)$ with which two neighboring pixels with grey levels i and j at a given

distance d and orientation θ occur on the image. The distances used are $d = \{1, 2, 3, 4\}$ pixels and the angles $\theta = \{0, 45, 90, 135\}^o$, thus creating 16 different GLCMs. From each computed GLCM we estimate the *Contrast*, *Correlation*, *Energy* and *Homogeneity* thus producing a 64-element feature vector. Furthermore, to investigate a possible relation between each pixel and its neighborhood, the ARM is used on the speckle image. This model assumes $\eta_{i,j}$ to be a 2D random variable where each pixel depends on its causal neighbors according to [12]:

$$\eta_{i,j} = \sum_{n,m}^{p,q} a_{n,m}\eta_{i-m,j-n} + u_{i,j} \quad (2)$$

where $a_{n,m}$ are the ARM coefficients to be estimated and $u_{i,j}$ are the residues. Considering a 1^{st} order model such that $(p, q) = (1, 1)$, we estimate 3 *ARM coefficients*. Alternatively, plaque texture can be studied using multi-level 2D wavelet decomposition. This technique consists in using low and high pass filters onto the approximation coefficients at level l in order to obtain the approximation at level $l + 1$, and the details in three orientations (horizontal, vertical, and diagonal). Here, decomposition is made along $l = 4$ levels. For each level, the *percentage of energy* for the approximation E_A as well as horizontal E_H, vertical E_V and diagonal E_D details is computed. Hence, a 13-element wavelet-based feature vector is obtained composed of 4 (E_H) + 4 (E_V) + 4 (E_D) + E_A.

Finally, each plaque is described by a feature vector $\mathbf{x}$ of 4 (Clinical) + 13 (Histogram) + 13 (RMM) + 4 (Rayleigh) + 80 (Texture) = 114 features.

A. Classification

In this paper, the AdaBoost (Adaptive Boosting) binary classifier [13] was used. AdaBoost designs a *strong* classifier by linearly combining a set of *weak* classifiers. The weak classifier used in this work is *decision stumps*, which has shown high performance for plaque classification [14]. At each round of the boosting algorithm, the classification error in classifying the training data set is minimized by selecting the best discriminative value of one feature in the vector $\mathbf{x}$. In addition, AdaBoost assigns at each round a weight to the selected feature which results in an automatic selection of the most discriminant features, given by the relative weight they assume at each round. Note that each feature can be selected more than one time: in that case, the sum of each weight for a specific feature is considered. Let us define N_P the number of plaques, N_F the number of features, $f = 1, \ldots, N_F$ the index of each feature, N_R the number of rounds by whose the computation has been repeated and $\alpha^f_{p,r}$ the weight assigned to the f^{th} feature. The normalized weight assigned by AdaBoost to each feature can be computed as:

$$w_f = \frac{1}{N_P N_R} \sum_{p=1}^{N_P} \sum_{r=1}^{N_R} \frac{\alpha^f_{p,r}}{\max\{\alpha^1_{p,r}, \ldots, \alpha^{N_F}_{p,r}\}} \quad (3)$$

This *feature selection* process can be applied to perform an *a-posteriori analysis* on the relevance and usefulness of the features used for plaque classification.

The classifier performance is assessed by means of the LOPO cross-validation technique, where the training set is built taking at each time all patients' data, except one, used for testing. Performance results are given in terms of Sensitivity: $Sens = \frac{TP}{TP+FN}$, Specificity: $Spec = \frac{TN}{TN+FP}$, Precision: $Prec = \frac{TP}{TP+FP}$ and Accuracy: $Acc = \frac{TP+TN}{TP+TN+FP+FN}$, where TP = True Positive, TN = True Negative, FP = False Positive and FN = False Negative.

III. EXPERIMENTAL RESULTS

In this section we present two types of results: (i) the classification performance using the proposed framework and (ii) analysis of the relevance of the features used for discriminating between symptomatic and asymptomatic plaques.

A. Classifiers Performance

In order to study the classification performance under different conditions, the classifier is trained with 5 different feature sets, considering: clinical information ($F.1$), clinical information and histogram features ($F.2$), all features except clinical information ($F.4$) and finally considering all the features ($F.5$). Moreover, we define a feature set $F.3$ which results from the computation of histogram and texture features from normalized BUS images, thus discarding the information contained on the de-speckled and speckle images. The 5 feature sets are used to classify the plaques of the database according to the LOPO technique. Classification performance is shown in Fig. 4 while a detailed description is given in Table I.

The following observations can be made: first, the clinical information ($F.1$) used is not enough *per se* for discriminating between symptomatic and asymptomatic plaques; the combination of $F.1$ with histogram features extracted from the normalized image ($F.2$) in general improves classification, although the identification of symptomatic plaques ($Sens$) is still relatively weak. Moreover, in order to investigate the usefulness of other sources of information, such as the de-speckled and speckle images for plaque classification, we compare the classification results obtained with $F.3$ and $F.5$: accuracy and sensitivity results are substantially improved from $F.3$ to $F.5$ showing that it is preferable to use echo-morphology and texture parameters extracted from the speckle-free and speckle images, rather than computing such features on the normalized image. In addition, the classifier $F.4$, which exclusively considers "image" features outperforms the classifier $F.1$, which does not states that clinical parameters are not important but that increasing relevance should be given to features obtained from image processing. Finally, the classification performance obtained with the total feature set ($F.5$) is the best among the studied cases, with 100% sensitivity for detecting symptomatic plaques.

B. Feature Analysis

In Fig. 5 the normalized weights assigned by AdaBoost during classification are shown when the feature sets $F.4$ and $F.5$ are used. Considering the feature set which produces the best classification results ($F.5$), it is observed that more relevance is given to clinical information, such as *evidence of plaque disruption* (feature #1), the *degree*

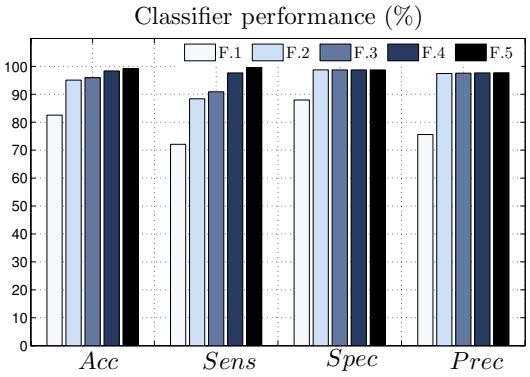

Fig. 4. Plaque classification using different feature sets.

TABLE I

LOPO (%)	$F.1$	$F.2$	$F.3$	$F.4$	$F.5$
Acc	82.54	95.08	95.94	98.36	99.18
$Sens$	72.09	88.37	90.91	97.67	100.00
$Spec$	87.95	98.73	98.73	98.73	98.73
$Prec$	75.61	97.44	97.56	97.67	97.73

of stenosis (#3), *plaque echo-structure appearance* (#4) and histogram features, such as *mean of grey values* (#5) and *kurtosis* (#9); surprisingly, the *median* (#6), which is used in several studies, is not selected by this classifier. Additionally, significant weights are assigned specifically to *RMM features*, *mean of Rayleigh values*, *GLCM*-based and *Wavelet* -based features, which strongly motivate their use for plaque classification. Moreover, a similar analysis is made when the feature set $F.4$ was applied for training the classifier. This analysis is justified by the fact that this feature set only considers features which were automatically extracted from the processed images. As expected, there is a re-distribution of the feature weights, where the relevance of the features increases in general. Note that, in this case, the *ARM*-based features are also considered relevant for classification. This fact determines that the increased importance given by the classifier to other image-based parameters compensates the lack of clinical information ($F.1$), providing even better classification results (cf. Table I).

IV. CONCLUSIONS

In this paper it was proposed a plaque classification framework for identifying symptomatic plaques. This method adds to the typical clinical information available, a set of features extracted from normalized, eRF, de-speckled and speckle estimated images of the plaque.

It has been shown that the use of such features improves the classification performance obtained when using uniquely clinical and histogram information, up to 99.18% accuracy and 100% sensitivity. Moreover, the speckle image, obtained after de-speckling, is a suitable source for texture information since the features extracted from this source ($F.4$) yield better classification performance when compared to the same features extracted from the normalized image ($F.3$).

Feature analysis reinforce the importance of fusing clinical information with echo-morphology and texture parameters for an accurate identification of symptoms in plaques.

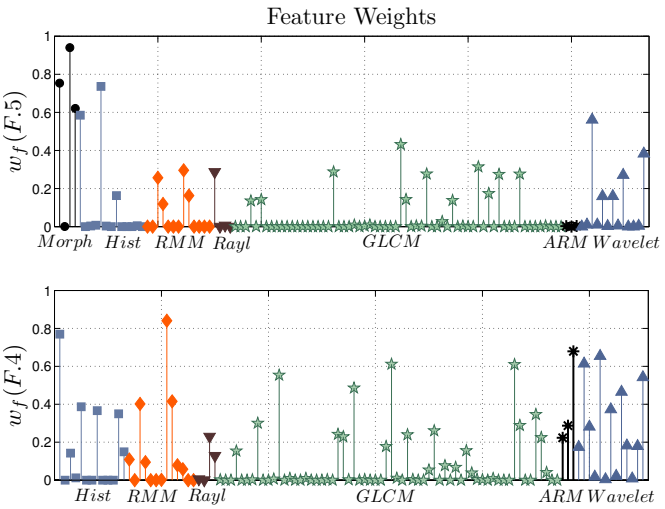

Fig. 5. Distribution of feature weights w_f for training sets $F.5$ and $F.4$.

REFERENCES

[1] North American Symptomatic Carotid Endarterectomy Trial Collaborators, "Benefit of carotid endarterectomy in patients with symptomatic moderate or severe stenosis," *New England Journal of Medicine*, vol. 339, no. 20, pp. 1445–1453, 1998.

[2] European Carotid Surgery Trialist's Collaborative Group, "Randomised trial of endarterectomy for recently symptomatic carotid stenosis: Final results of the mrc european carotid surgery trial (ecst)," *Lancet*, vol. 339, pp. 1379–1387, 1998.

[3] N. El-Barghouty, T. Levine, S. Ladva, A. Flanagan, and A. Nicolaides, "Histological verification of computerised carotid plaque characterisation," *Eur J Vasc Endovasc Surg.*, vol. 11, no. 4, pp. 414–416, 1996.

[4] T. Elatrozy, A. Nicolaides, T. Tegos, and M. Griffin, "The objective characterization of ultrasonic carotid plaque features," *Eur J Vasc Endovasc Surg*, vol. 16, pp. 223–230, 1998.

[5] L. Pedro, J. Fernandes, M. Pedro, I. Gonçalves, and N. Dias, "Ultrasonographic risk score of carotid plaques," *Eur Journal of Vasc and Endovasc Surg*, vol. 24, pp. 492–498, December 2002.

[6] C. Christodoulou, C. Pattichis, M. Pantziaris, and A. Nicolaides, "Texture-based classification of atherosclerotic carotid plaques," *IEEE Transactions on Medical Imaging*, vol. 22, no. 7, 2003.

[7] S. G. Mougiakakou, S. Golemati, I. Gousias, A. N. Nicolaides, and K. S. Nikita, "Computer-aided diagnosis of carotid atherosclerosis based on ultrasound image statistics, laws' texture and neural networks," *Ultras Med Biol*, vol. 33, no. 1, pp. 26–36, Jan 2007.

[8] J. M. Thijssen, "Ultrasonic speckle formation, analysis and processing applied to tissue characterization," *Pattern Recognition Letters*, vol. 24, no. 4-5, pp. 659–675, 2003.

[9] J. Seabra, J. Xavier, and J. Sanches, "Convex ultrasound image reconstruction with log-euclidean priors," in *Proceedings EMBC 2008*. Vancouver, Canada: IEEE Engineering in Medicine and Biology Society, 2008.

[10] J. Seabra and J. Sanches, "Modeling log-compressed ultrasound images for radio frequency signal recovery," in *Proceedings EMBC 2008*. Vancouver, Canada: IEEE Engineering in Medicine and Biology Society, 2008.

[11] J. Seabra, J. Sanches, F. Ciompi, and P. Radeva, "Ultrasonographic plaque characterization using a Rayleigh Mixture Model," in *Proceedings ISBI 2010*. Rotterdam, The Netherlands: IEEE Engineering in Medicine and Biology Society, 2010, to appear. [Online]. Available: http://users.isr.ist.utl.pt/~jseabra/papers/isbi_RMM.pdf

[12] K. Wear, R. Wagner, and B. Garra, "A comparison of autoregressive spectral estimation algorithms and order determination methods in ultrasonic tissue characterization," *IEEE Transactions on Ultrasonics, Ferroelectrics and Frequency Control*, vol. 42, no. 4, pp. 709–716, July 1995.

[13] R. Schapire, "The boosting approach to machine learning: An overview," 2001.

[14] F. Ciompi, O.Pujol, O. R. Leor, C. Gatta, A. S. Vida, and P. Radeva, "Enhancing in-vitro ivus data for tissue characterization," *Lecture Notes in Computer Science*, vol. 5524, pp. 241–248, 2009.